Enhanced Electrocatalytic Methanol Oxidation using $Ti_3C_2T_x$ MXenes-Based Composites Synthesized via FeF_3/HCl Etching Environment

Norulsamani Abdullah[1*], Tan Kim Han[1], Md Abu Zaed[1], Nurul Atiqah Izzati Md Ishak[2] and R. Saidur[1,3]

[1] Research Center for Nano-Materials and Energy Technology (RCNMET), Faculty of Engineering and Technology, Sunway University, No. 5, Jalan Universiti, Bandar Sunway, 47500 Selangor Darul Ehsan, Malaysia.
[2] Research Centre for Carbon Dioxide Capture and Utilisation (CCDCU), Faculty of Engineering and Technology, Sunway University, No. 5, Jalan Universiti, Bandar Sunway, 47500 Selangor Darul Ehsan, Malaysia
[3] School of Engineering, Lancaster University, Lancaster, LA1 4YW, United Kingdom.

[*]E-mail: nabdullah@sunway.edu; norulsamani@gmail.com

Abstract. MXenes, a rapidly emerging class of two-dimensional materials, have gained significant attention as catalysts in fuel cell technology due to their exceptional electrical conductivity, and large surface area. The ability of MXenes to modify surface terminations and incorporate various transition metals further enhances their catalytic activity. These characteristics make MXenes particularly effective in facilitating key electrochemical reactions, such as methanol oxidation and oxygen reduction, which are critical for the efficiency of direct methanol fuel cells. This study presents the synthesis and characterization of $Ti_3C_2T_x$ MXenes using a novel FeF_3/HCl etching method, followed by the deposition of PtRu bimetal ($PtRu/Ti_3C_2T_x$_FeF_3) to enhance electrocatalytic activity for methanol oxidation reactions (MOR). The unique etching environment facilitates the efficient removal of aluminum layers from the MAX phase, leading to high-purity $Ti_3C_2T_x$ MXenes with desirable surface terminations. The $Ti_3C_2T_x$ MXene-based composite was characterized through various analytical techniques, including field emission scanning electron microscopy (FESEM), x-ray photoelectron spectroscopy (XPS), and cyclic voltammetry (CV). The resulting composites exhibit excellent of $PtRu/Ti_3C_2T_x$_FeF_3 composite electrocatalyst in MOR activity, where the catalyst loading of 0.4 $mgcm^{-2}$ produced the highest mass activity. Additionally, the FeF_3/HCl etching route outperformed conventional LiF/HCl etching agents, delivering ~4.7 times better in MOR activity. These findings underscore the potential of FeF_3/HCl-etched $Ti_3C_2T_x$ MXenes-based composites as promising materials for fuel cell applications and other energy-related processes.

Keywords: MXene, Etching environment, Electrocatalytic activity, Methanol oxidation

1. Introduction

MXene, a new class of two-dimensional (2D) transition metal carbides, nitrides, and carbonitrides, is a promising material for various applications, particularly in catalysis. Its excellent electronic conductivity, redox activity of surface metal atoms, and tunable properties make it highly effective [1]. MXenes consist of layers of transition metals (M elements) combined with carbon or nitrogen (X elements) and surface terminations like O, OH, F, or Cl (T_x elements), following the formula $M_{n+1}X_nT_x$ [2]. Over 50 types of MXenes have been developed, with $Ti_3C_2T_x$ MXene selected for this study due to its outstanding electrochemical performance [3].

MXenes are synthesized through selective etching, where A-layer atoms (such as Al, Si, or Ga) are removed from the precursor MAX phases, as shown in Figure 1. One of the most common methods for MXene synthesis is chemical etching, which requires etching agents. These agents selectively remove A-layer atoms, allowing the formation of MX layers with properties suited for applications like MOR activity. The choice of etching agents affects the surface chemistry, morphology, and composition of MXene sheets, influencing their electrochemical behavior [4]. Traditionally, hydrofluoric acid (HF) has been widely used for this process, but its toxicity and environmental impact have raised concerns. To address this, newer, safer etching agents such as LiF/HCl and NH_4HF_2 have been explored. In this study, FeF_3/HCl was chosen as the etching agent due to its relative safety, environmental friendliness, and the limited research on its potential for electrochemical applications. Although FeF_3 and HCl may still generate acidic byproducts, their use avoids direct handling of HF and more suitable for controlled synthesis settings. Nonetheless, we acknowledge that scaling up the FeF_3/HCl process requires careful consideration of waste management and gas emissions, for example HCl vapors and iron-containing residues. Future work should focus on optimizing the synthesis for greener practices, such as closed-loop acid recovery systems and post-treatment neutralization, to ensure environmental sustainability and safety at industrial scales.

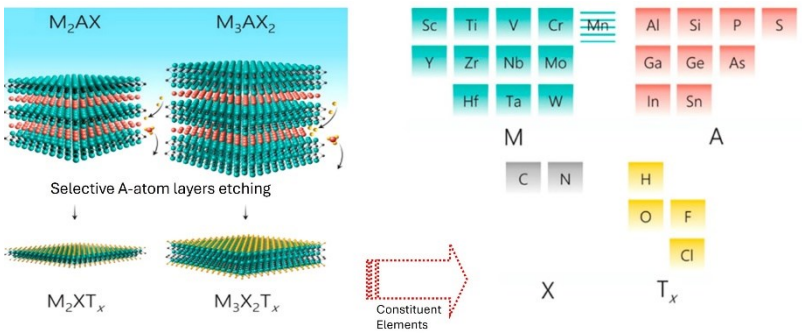

Figure 1. Illustration of MXenes synthesized from the MAX phase precursors, with the recent key elements involved in MAX phase and MXene research [5].

$Ti_3C_2T_x$ MXenes have gained attention as catalysts for the methanol oxidation reaction (MOR), the key anodic reaction in direct methanol fuel cells (DMFCs), due to their high catalytic activity, tunable surface chemistry, and simple synthesis. Their surface functional groups is expected to enhance catalyst deposition and electrochemical reactions, increasing active surface area and boosting DMFC performance [6]. MXenes are also well-suited for DMFCs' harsh conditions, such as acidic environments and high currents, making them ideal for improving cell efficiency. Recent studies, including those by Lan et al. [7], and Qin et al. [8], highlighted their potential in enhancing MOR activity.

This study builds upon our previous work on FeF_3/HCl-etched $Ti_3C_2T_x$ MXenes by integrating them with PtRu bimetallic catalysts to enhance electrocatalytic performance in the MOR [5]. While FeF_3/HCl etching has been previously explored, this work is the first to systematically investigate the effect of varying electrocatalyst loadings on the MOR activity of $Ti_3C_2T_x$-based composites synthesized through this route. The study conducted morphological, physicochemical, and electrochemical analyses using field emission scanning electron microscopy (FESEM) and x-ray photoelectron spectroscopy (XPS), and cyclic voltammetry (CV). Results show that the FeF_3/HCl-etched MXene-based composite exhibited ~4.7 times better electrocatalytic activity in MOR compared to MXene-based composite synthesized using the conventional LiF/HCl route. This demonstrates that FeF_3/HCl not only provides a safer alternative but also has strong potential to be used in electrochemical-based application.

2. Experimental

2.1 Synthesis of $Ti_3C_2T_x$ MXene via FeF_3/HCl etching route

$Ti_3C_2T_x$ MXene was synthesized using a modified acid etching method with FeF_3/HCl as the etching agent. First, 2 g of FeF_3 and 15 ml of 9 M HCl were mixed with 5 ml of deionized water for 15 minutes. Then, 1 g of Ti_3AlC_2 MAX phase was slowly added and stirred for 15 minutes at room temperature. The solution was continuously stirred for another 48 hours at 60°C. Next, the solution was repeatedly washed and centrifuged with deionized water. The final material was dried in a vacuum condition at 60°C for 12 hours and referred to as $Ti_3C_2T_x$_FeF_3 MXene, which will be used in this study.

2.2 Synthesis of PtRu/$Ti_3C_2T_x$_FeF_3 electrocatalyst

The PtRu catalysts were deposited onto $Ti_3C_2T_x$ MXene using a solvothermal method. A mixture of 50 mL isopropyl alcohol, 50 mL deionized water, and 80 wt% MXene was sonicated for 30 minutes at room temperature. Pt and Ru precursors in a 1:1 ratio (H_2PtCl_6 and $RuCl_3$) were then added and stirred for another 30 minutes. The solution was transferred to an autoclave and heated at 120°C for 24 hours. After cooling, the mixture was filtered, washed with deionized water, and dried under vacuum at 70°C overnight. The final PtRu/$Ti_3C_2T_x$_FeF_3 electrocatalyst was then ground into a fine powder.

2.3 Physicochemical and electrochemical assessment of $Ti_3C_2T_x$ MXene and PtRu/$Ti_3C_2T_x$_FeF_3

A systematic characterization strategy was adopted to evaluate the morphological, and surface chemical properties of the synthesized electrocatalysts. FESEM (Hitachi SU8010, Japan) revealed surface morphology and catalyst dispersion, while XPS analysis (Kratos – Axis Ultra DLD) was conducted to examine surface chemistry and elemental of the materials.

The electrocatalytic activity was then assessed through CV, to assess the impact of catalyst loading and FeF_3/HCl etching route towards catalytic behaviour in MOR. The CV is conducted using a potentiostat/galvanostat (Interface 1010E, Gamry Instruments, USA) with a three-electrode system: glassy carbon as the working electrode, Ag/AgCl as the reference electrode, and Pt as the counter electrode. The sample's ink was prepared by mixing 5 mg of sample powder with a solution of isopropyl alcohol, deionized water and 5wt% Nafion solution in a 5:5:1 ratio, followed by sonication for 1 hour. Then, 4 µL of the ink was pipetted onto the 3 mm surface of the working electrode, dried at room temperature for 1 hour, and further dried at 65°C for 30 minutes before electrochemical measurements.

3. Result and Discussion

3.1 Physicochemical characterization of $Ti_3C_2T_x$_FeF_3 and PtRu/$Ti_3C_2T_x$_FeF_3

The surface morphology of the synthesized $Ti_3C_2T_x$_FeF_3 and its composite, PtRu/$Ti_3C_2T_x$_FeF_3, was analyzed using FESEM, as shown in Figure 2. The $Ti_3C_2T_x$_FeF_3 in Figure 2 (a) displays a flaky, layered structure resembling a 'wet book sheet,' consistent with the typical 2D MXene morphology reported in the literature [9], confirming successful fabrication. The sheets appear densely packed with no signs of delamination, in line with previous studies [10]. Figure 2 (b) shows the PtRu/$Ti_3C_2T_x$_FeF_3 electrocatalyst, where nanoparticles (Pt and Ru) are evenly deposited across the MXene structure, including the interlayer spaces. Elemental mapping in Figure 2 (c) confirms the uniform distribution of Pt and Ru on the $Ti_3C_2T_x$_FeF_3 surface, which is expected to enhance active site availability, electron transfer, surface area, mass transport, and synergistic effects between the MXene and bimetals—key factors for high catalytic activity.

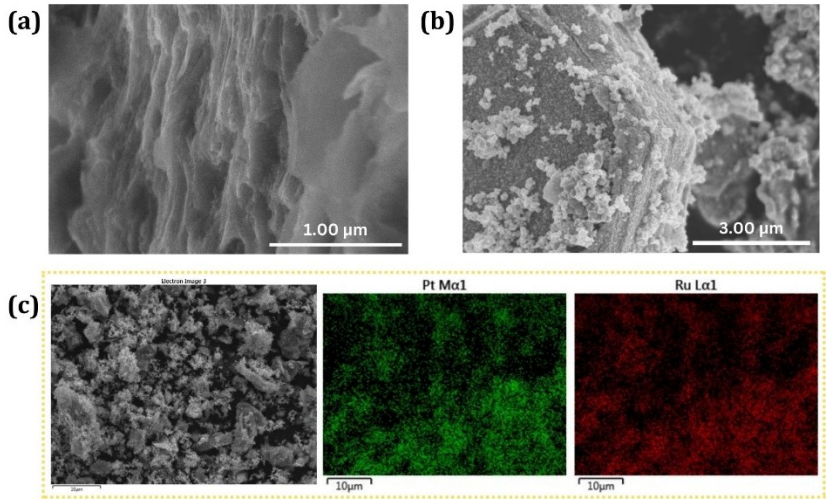

Figure 2. FESEM images of (a) $Ti_3C_2T_x$_FeF_3 at 50kX magnification, (b) PtRu/$Ti_3C_2T_x$_FeF_3 at 15kX magnification; and (c) elemental mapping via SEM for PtRu/$Ti_3C_2T_x$_FeF_3.

Figure 3 show the XPS survey spectra for $Ti_3C_2T_x$_FeF_3 and PtRu/$Ti_3C_2T_x$_FeF_3, identifying the surface chemistry and elemental composition of the materials. In Figure 3 (a), the wide survey spectra show distinct elemental peaks for C 1s, Ti 2p, O 1s, Fe 2p, and F 1s in $Ti_3C_2T_x$_FeF_3. In the case of PtRu/$Ti_3C_2T_x$_FeF_3, additional peaks for Pt 4f and Ru 3d are observed, confirming the successful deposition of Pt and Ru onto the surface. The presence of Fe in both samples is attributed to the FeF_3/HCl etching agent used during synthesis.

Figures 3 (b–e) present the high-resolution spectra and peak fitting for $Ti_3C_2T_x$_FeF_3. In the C 1s region of $Ti_3C_2T_x$_FeF_3, six peaks are observed at binding energies of approximately 278.9 eV, 280.5 eV, 281.9 eV, 283.1 eV, 284.4 eV, and 286 eV, corresponding to C-Ti-T_x, O-H, C-C, C-O, C=O, and C-F_{2+x}, respectively. The Ti 2p region exhibits nine peaks at 452.3 eV, 458 eV, 453.5 eV, 459.4 eV, 454.7 eV, 461.1 eV, 456.1 eV, 464.2 eV, and 462.4 eV, indicating the presence of C-Ti-C, C-Ti-O, C-Ti-(O, F), C-Ti-F, and $TiO_{2-x}F_{2x}$ bonds. In the O 1s region, peaks are centered around 527.1 eV, 529.8 eV, 528.6 eV, and 531.3 eV, corresponding to C-Ti-O, $TiO_{2-x}F_{2x}$, and C-Ti-OH. The F 1s region shows three peaks at approximately 682 eV, 683 eV, and 684.3 eV, attributed to C-Ti-F_x, Al-F_x, and C-F_{2+x}, respectively. The presence of these elements in $Ti_3C_2T_x$_FeF_3 results from the incomplete

etching process of the FeF_3/HCl etching agent. Overall, the peak fitting in the C 1s, Ti 2p, O 1s, and F 1s regions confirms the formation of several terminal groups, including oxide (–O–), hydroxyl (–OH), and fluoride (–F), on the $Ti_3C_2T_x$_FeF_3 surface.

The XPS spectra of the PtRu/$Ti_3C_2T_x$_FeF_3 composite electrocatalyst reveal distinct peaks for Pt 4f and Ru 3d, confirming successful bimetal deposition. The presence of other elements, such as Ti 2p and O 1s, remains consistent with $Ti_3C_2T_x$_FeF_3. However, the F 1s peaks disappear in PtRu/$Ti_3C_2T_x$_FeF_3, likely due to the replacement of unstable F-terminations with more stable Pt and Ru bonds during deposition, as noted by Zhao et al. [11]. Additionally, an increase in C 1s peak intensity is observed, attributed to the overlap with Ru 3d binding energies (279-288 eV). The Ti 2p and O 1s peaks also shift by 0.4 to 0.6 eV, indicating stronger electronic interactions between Pt, Ru, and the $Ti_3C_2T_x$_FeF_3 structure, similar to findings by Kruse et al. [12].

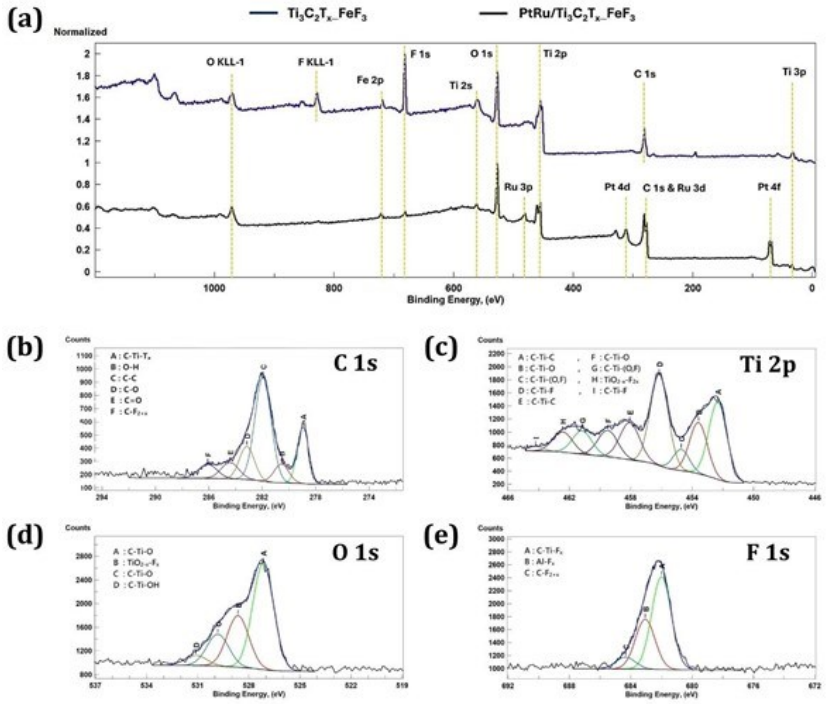

Figure 3. Wide XPS survey spectra for (a) $Ti_3C_2T_x$_FeF_3 and PtRu/$Ti_3C_2T_x$_FeF_3. XPS high-resolution and peak fitting spectra for $Ti_3C_2T_x$_FeF_3 at regions of (b) C 1s, (c) Ti 2p, (d) O 1s, and (e) F 1s.

3.2 Electrochemical measurement of $Ti_3C_2T_x$_FeF_3 and PtRu/$Ti_3C_2T_x$_FeF_3

The electrocatalytic activity of the synthesized $Ti_3C_2T_x$_FeF_3 and PtRu/$Ti_3C_2T_x$_FeF_3 was evaluated through CV measurements in the methanol oxidation reaction (MOR) using different catalyst loadings (0.2, 0.4, 0.6 mg cm^{-2}), with annotation of $Ti_3C_2T_x$_FeF_3 (0.2). The measurements were conducted in a solution of 1 M CH_3OH and 0.5 M H_2SO_4 under anodic half-cell conditions, with oxygen-free content. The CV curves were scanned in the potential range of -0.2 to 1.0 V vs. Ag/AgCl at a scan rate of 20 mV s^{-1}. Figure 4 presents the CV curves for $Ti_3C_2T_x$_FeF_3 and PtRu/$Ti_3C_2T_x$_FeF_3 at varying catalyst loadings, with an inset providing an enlarged view of the $Ti_3C_2T_x$_FeF_3 curves. The forward anodic current peak (I_f) corresponding to CH_3OH oxidation and the reverse anodic peak current (I_b) are clearly visible. Overall, PtRu/$Ti_3C_2T_x$_FeF_3 demonstrates

higher MOR activity than $Ti_3C_2T_x$_FeF_3, attributed to the incorporation of PtRu into the $Ti_3C_2T_x$_FeF_3 structure, which enhances the electrocatalytic performance compared to the bare $Ti_3C_2T_x$_FeF_3 [9].

Notably, PtRu/$Ti_3C_2T_x$_FeF_3 with a catalyst loading of 0.4 mg cm^{-2} demonstrated the highest mass activity, which was 1.4 and 1.9 times greater than those with catalyst loadings of 0.6 mg cm^{-2} and 0.2 mg cm^{-2}, respectively. While the catalytic activity increased with higher catalyst loading, it started to decline after reaching 0.4 mg cm^{-2}, consistent with the CV results for $Ti_3C_2T_x$_FeF_3. At 0.2 mg cm^{-2}, the catalyst layer is too thin, resulting in an insufficient number of active sites for methanol oxidation, which limits the overall reaction rate. Increasing the loading to 0.4 mg cm^{-2} enhances the density of active sites and improves the contact between catalyst and electrode, thereby facilitating better electron transfer and mass transport, which leads to significantly higher catalytic activity. However, beyond this optimal point, such as at 0.6 mg cm^{-2}, results in a performance decline. This is attributed to the formation of a thicker catalyst layer, which can lead to particle agglomeration, hinder reactant diffusion, and limit access to inner active sites. Although agglomeration was not directly observed, this trend is well-documented in previous studies [13, 14], where excessive loading has been shown to reduce electrochemical performance due to transport limitations and reduced effective surface area. These findings underscore the importance of optimizing catalyst loading to balance catalytic activity, electrical conductivity, and mass transport efficiency [15].

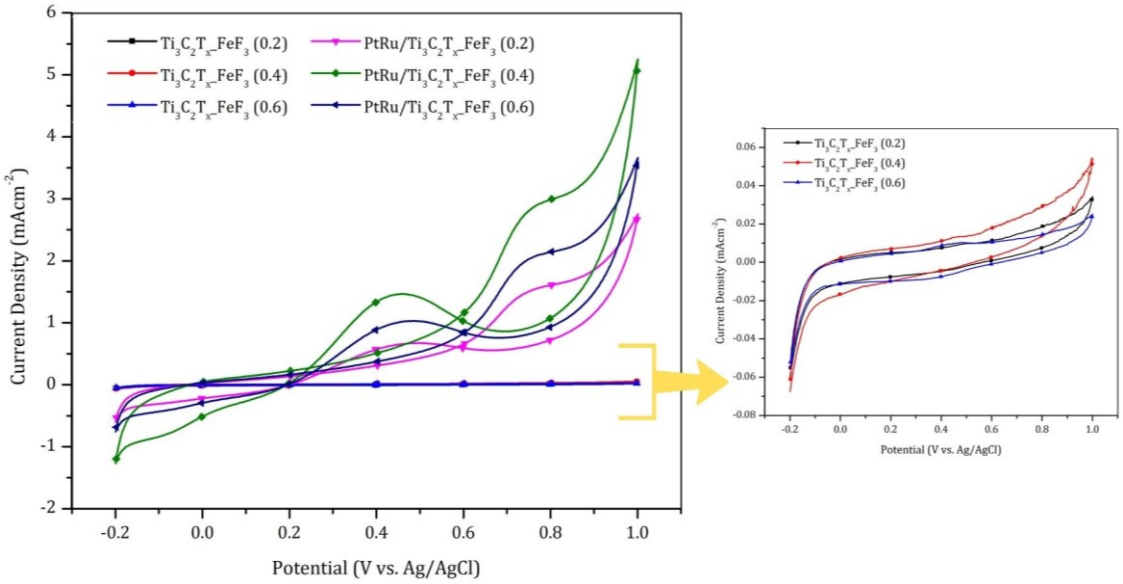

Figure 4. CV curves of $Ti_3C_2T_x$_FeF_3 and PtRu/$Ti_3C_2T_x$_FeF_3 at various catalyst loadings (0.2, 0.4, 0.6 mg cm^{-2}) in a solution of 1.0 M CH_3OH and 0.5 M H_2SO_4.

To assess the impact of the FeF_3/HCl etching environment on the electrocatalytic performance, a comparison was made with pristine $Ti_3C_2T_x$ synthesized using the LiF/HCl route, as reported in our previous study [5]. The pristine $Ti_3C_2T_x$ prepared via LiF/HCl exhibited a lower MOR activity, with specific activity of approximately 0.62 $mAcm^{-2}$ under similar experimental conditions. In contrast, the PtRu/$Ti_3C_2T_x$_0.4 composite synthesized in this study via the FeF_3/HCl route achieved a significantly enhanced specific activity of 2.91 $mAcm^{-2}$, demonstrating ~4.7-fold increase. These findings confirm that the FeF_3/HCl route not only offers a more environmentally

friendly alternative to conventional methods but also yields superior electrocatalytic performance compared to the previously studied pristine $Ti_3C_2T_x$ prepared via LiF/HCl.

The MOR activity of the synthesized PtRu/$Ti_3C_2T_x$_FeF_3 composite electrocatalyst, produced via the FeF_3/HCl etching method, is also compared with other $Ti_3C_2T_x$ MXene-based electrocatalysts synthesized using different etching agents, as shown in Table 1. The results show that the specific activity of PtRu/$Ti_3C_2T_x$_FeF_3 is the highest among all compared electrocatalysts. Specifically, its activity is approximately 1.5 and 1.7 times higher than those synthesized via the traditional HF and commonly used LiF/HCl routes, respectively. This enhanced performance can be attributed to the intercalation of Fe atoms, as confirmed by XPS analysis, which promotes faster electron transfer and ion diffusion, providing access to more active sites and improving reaction kinetics [16]. Additionally, the Fe intercalation is suggested to increase the catalyst's surface area, with Fe acting as a conductive support, further boosting MOR activity [17]. The Fe atoms from the FeF_3/HCl route may also contribute to the stability of the MXene structure. When combined with the state-of-the-art PtRu catalyst, the etching method influences the mass activity, correlating with the strength of the etching agent and the resulting termination groups attached to the MXene structure [18]. This comparison also highlights the shift in research towards more environmentally friendly etching methods, with the LiF/HCl route being favored over the hazardous HF route. Although this comparison is not a perfect benchmark—due to differences in factors such as metal type, electrolyte composition, and scan rates—the performance gap in MOR activity remains clear.

Table 1. Comparative analysis of MOR activity in $Ti_3C_2T_x$ MXene-based electrocatalysts from different studies using various etching routes.

Electrocatalyst	Etching Route	Specific Activity ($mAcm^{-2}$)	References
PtRu/$Ti_3C_2T_x$_FeF_3	FeF_3/HCl	2.91	This study
$NiMoS_2$-15/MXene	HF	1.93	[19]
Pt/$Ti_3C_2T_x$	HF	1.14	[20]
PtRu/MXene-G	LiF/HCl	1.75	[21]
Pt NWs/MX	LiF/HCl	1.6	[22]
Pt/$(RGO)_3$-$(Ti_3C_2T_x)_7$	LiF/HCl	1.5	[23]
Pd NSs/MXene	LiF/HCl	1.3	[24]
PtRu/MXene	NH_4HF_2	1.19	[25]

The FeF_3/HCl method not only enhances electrochemical performance but also presents a more sustainable approach, considering that Fe is the fourth most abundant element in the Earth's crust, unlike the limited availability of lithium. Utilizing MXenes as a catalyst support, combined with bimetallic Pt and Ru, offers significant improvements in catalytic activity, positioning this material as a viable alternative to commercial electrocatalysts in DMFC

applications. These findings mark an important step in advancing multifunctional nanomaterials for cleaner, more efficient energy sources, contributing to global sustainability efforts.

4. Conclusion

This study successfully synthesized $Ti_3C_2T_x$ MXenes-based composites electrocatalyst via a novel FeF_3/HCl etching environment. By integrating $Ti_3C_2T_x$ MXenes with Pt and Ru bimetal particles, the materials were well-characterized, and their electrochemical performance evaluated. The results confirmed the formation of MXenes with layered morphologies and uniform distribution of Pt and Ru particles. XPS analysis also highlighted the successful deposition of these metals and the intercalation of Fe atoms. The series of electrochemical assessment is confirmed the excellent of PtRu/$Ti_3C_2T_x$_FeF_3 composite electrocatalyst in MOR activity. The optimized catalyst loading of 0.4 mgcm^{-2} produced the highest mass activity, showcasing the importance of balancing catalyst loading for achieving maximum catalytic efficiency. Additionally, the FeF_3/HCl etching route outperformed conventional LiF/HCl etching agents, delivering ~4.7 times better in MOR activity. This is due to the enhanced electron transfer, ion diffusion, and increased active sites facilitated by Fe intercalation. This approach also presents a more environmentally friendly and sustainable alternative to the hazardous HF etching route, which commonly used in MXene synthesis. By utilizing abundant materials like Fe and adopting a more sustainable synthesis process, this work marks a critical step toward advancing nanomaterial-based electrocatalysts for affordable and clean energy applications. Future research should focus on further optimizing synthesis parameters and exploring the scalability of this method for practical energy conversion devices.

Acknowledgement

The authors sincerely thank Sunway University for their support through the Research Accelerator Grant Scheme, GRTIN-RAG(02)-RCNMET-03-2025, which was instrumental in enabling this research.

References

[1] M. Khazaei, A. Mishra, N.S. Venkataramanan, A.K. Singh, S. Yunoki, Recent advances in MXenes: From fundamentals to applications, Current Opinion in Solid State and Materials Science, 23 (2019) 164-178.
[2] Y. Gogotsi, B. Anasori, The rise of MXenes, MXenes, Jenny Stanford Publishing2023, pp. 3-11.
[3] N. Abdullah, R. Saidur, A.M. Zainoodin, N. Aslfattahi, Optimization of electrocatalyst performance of platinum–ruthenium induced with MXene by response surface methodology for clean energy application, Journal of Cleaner Production, 277 (2020) 123395.
[4] Y.-J. Kim, S.J. Kim, D. Seo, Y. Chae, M. Anayee, Y. Lee, Y. Gogotsi, C.W. Ahn, H.-T. Jung, Etching mechanism of monoatomic aluminum layers during MXene synthesis, Chemistry of Materials, 33 (2021) 6346-6355.
[5] N. Abdullah, N.A.I.M. Ishak, K. Tan, M. Zaed, R. Saidur, A. Pandey, Investigating the impact of various etching agents on Ti3C2Tx MXene synthesis for electrochemical energy conversion, FlatChem, 47 (2024) 100730.
[6] S.G. Peera, C. Liu, J. Shim, A.K. Sahu, T.G. Lee, M. Selvaraj, R. Koutavarapu, MXene (Ti3C2Tx) supported electrocatalysts for methanol and ethanol electrooxidation: A review, Ceramics International, 47 (2021) 28106-28121.
[7] Y. Lan, H. He, C. Liu, J. Qin, L. Luo, F. Zhu, Y. Zhao, J. Zhang, L. Yang, H. Huang, Ultrasmall Pd nanocrystals confined into Co-based metal organic framework-decorated MXene nanoarchitectures for efficient methanol electrooxidation, Journal of Power Sources, 603 (2024) 234438.
[8] J. Qin, H. Huang, J. Zhang, F. Zhu, L. Luo, C. Zhang, L. Yang, Q. Jiang, H. He, Stereoassembly of ultrasmall Rh-decorated zeolite imidazolate framework–MXene heterostructures for boosted methanol oxidation reaction, Journal of Materials Chemistry A, 11 (2023) 2848-2856.

[9] N. Abdullah, S. Rahman, A.M. Zainoodin, N. Aslfattahi, Comparative study for electrochemical and Single-Cell performance of a novel MXene-Supported Platinum–Ruthenium catalyst for Direct methanol fuel cell application, Journal of Electroanalytical Chemistry, 925 (2022) 116884.
[10] M. Benchakar, L. Loupias, C. Garnero, T. Bilyk, C. Morais, C. Canaff, N. Guignard, S. Morisset, H. Pazniak, S. Hurand, One MAX phase, different MXenes: a guideline to understand the crucial role of etching conditions on Ti3C2Tx surface chemistry, Applied Surface Science, 530 (2020) 147209.
[11] D. Zhao, R. Zhao, S. Dong, X. Miao, Z. Zhang, C. Wang, L. Yin, Alkali-induced 3D crinkled porous Ti 3 C 2 MXene architectures coupled with NiCoP bimetallic phosphide nanoparticles as anodes for high-performance sodium-ion batteries, Energy & Environmental Science, 12 (2019) 2422-2432.
[12] N. Kruse, S. Chenakin, XPS characterization of Au/TiO2 catalysts: Binding energy assessment and irradiation effects. Applied Catalysis A: General, 391(2011) 367-376.
[13] M.R. Smith, C.B. Martin, S. Arumuganainar, A. Gilman, B.E. Koel, M.L. Sarazen, Mechanistic elucidations of highly dispersed metalloporphyrin metal-organic framework catalysts for CO2 electroreduction. Angewandte Chemie International Edition, 62(2023) e202218208.
[14] J. Sun, F. Liu, U. Salahuddin, M. Wu, C. Zhu, X. Lu, B. Zhang, B. Zhao, Z. Xie, Y. Ding, D. Li, Optimization and understanding of ZnO nanoarray supported Cu-ZnO-Al2O3 catalyst for enhanced CO2-methanol conversion at low temperature and pressure. Chemical Engineering Journal, 455 (2025) 140559.
[15] N. Abdullah, S.K. Kamarudin, L. Shyuan, N. Karim, Synthesis and optimization of PtRu/TiO2-CNF anodic catalyst for direct methanol fuel cell, International Journal of Hydrogen Energy, 44 (2019) 30543-30552.
[16] A. Raveendran, M. Chandran, M.R. Siddiqui, S.M. Wabaidur, M. Eswaran, R. Dhanusuraman, Layer-by-Layer Assembly of CTAB-rGO-Modified MXene Hybrid Films as Multifunctional Electrodes for Hydrogen Evolution and Oxygen Evolution Reactions, Supercapacitors, and DMFC Applications, ACS Omega, 8 (2023) 34768-34786.
[17] K.R.G. Lim, A.D. Handoko, S.K. Nemani, B. Wyatt, H.-Y. Jiang, J. Tang, B. Anasori, Z.W. Seh, Rational design of two-dimensional transition metal carbide/nitride (MXene) hybrids and nanocomposites for catalytic energy storage and conversion, ACS Nano, 14 (2020) 10834-10864.
[18] B. Anasori, M.R. Lukatskaya, Y. Gogotsi, 2D metal carbides and nitrides (MXenes) for energy storage, MXenes, Jenny Stanford Publishing2023, pp. 677-722.
[19] M. Chandran, A. Raveendran, M. Vinoba, B.K. Vijayan, M. Bhagiyalakshmi, Nickel-decorated MoS2/MXene nanosheets composites for electrocatalytic oxidation of methanol, Ceramics International, 47 (2021) 26847-26855.
[20] Y. Wang, J. Wang, G. Han, C. Du, Q. Deng, Y. Gao, G. Yin, Y. Song, Pt decorated Ti3C2 MXene for enhanced methanol oxidation reaction, Ceramics International, 45 (2019) 2411-2417.
[21] Q. Zhang, Z. Deng, H. He, G. Ying, H. Huang, Immobilizing ultrafine PtRu alloy nanoparticles onto 3D interconnected MXene-graphene frameworks for highly efficient methanol oxidation, Ceramics International, 50 (2024) 16443-16451.
[22] W. Meng, H. He, L. Yang, Q. Jiang, B. Yuliarto, Y. Yamauchi, X. Xu, H. Huang, 1D-2D hybridization: nanoarchitectonics for grain boundary-rich platinum nanowires coupled with MXene nanosheets as efficient methanol oxidation electrocatalysts, Chemical Engineering Journal, 450 (2022) 137932.
[23] C. Yang, Q. Jiang, W. Li, H. He, L. Yang, Z. Lu, H. Huang, Ultrafine Pt nanoparticle-decorated 3D hybrid architectures built from reduced graphene oxide and MXene nanosheets for methanol oxidation, Chemistry of Materials, 31 (2019) 9277-9287.
[24] H. Huang, D. Xiao, Z. Zhu, C. Zhang, L. Yang, H. He, J. You, Q. Jiang, X. Xu, Y. Yamauchi, A 2D/2D heterojunction of ultrathin Pd nanosheet/MXene towards highly efficient methanol oxidation reaction: the significance of 2D material nanoarchitectonics, Chemical Science, 14 (2023) 9854-9862.
[25] N. Abdullah, R. Saidur, A.M. Zainoodin, K.H. Tan, A.K. Pandey, Enhancing methanol oxidation reaction with platinum–ruthenium embedded MXene: Synthesis, characterization, and electrochemical properties, Journal of Physics and Chemistry of Solids, 180 (2023) 111434.